International Journal of Nanomedicine

Dovepress
open access to scientific and medical research

Open Access Full Text Article

ORIGINAL RESEARCH

Nanoparticle delivery and combination therapy of gambogic acid and all-trans retinoic acid

This article was published in the following Dove Press journal:
International Journal of Nanomedicine
10 July 2014
Number of times this article has been viewed

Jing Yao
Yuanke Li
Xiaojing Sun
Fatima Zohra Dahmani
Hongpan Liu
Jianping Zhou

State Key Laboratory of Natural Medicines, China Pharmaceutical University, Nanjing, People's Republic of China

Abstract: In order to enhance the in vivo codelivery efficiency of gambogic acid (GA) and all-trans retinoic acid (ATRA), our strategy was to entrap GA in the self-assembled nanoparticles based on amphiphilic hyaluronic acid (HA)-ATRA (HRA) conjugate. In this way, GA and ATRA were loaded simultaneously in a nanocarrier and codelivered into the tumor cell through HA receptor-mediated endocytosis. GA-loaded HRA nanoparticles (GA-HRA) were prepared by a dialysis method, and their physicochemical characteristics were investigated as well. GA-HRA exhibited a high drug loading capacity (31.1%), had a particle size in the range of 100–150 nm, and good biocompatibility. HRA nanoparticles were effectively internalized by MCF-7 cells and translocated into the nucleus in a time-dependent manner. The in vivo imaging analysis demonstrated that the fluorescent signals in the tumor were markedly increased with DiR-loaded nanoparticles after intravenous administration compared to free DiR solution, suggesting it has excellent tumor targeting properties. More importantly, GA-HRA exhibited excellent in vivo efficacy with dramatically reduced toxicity. In conclusion, with the assistance of HRA nanoparticles, GA and ATRA can successfully realize an effective combination chemotherapy as well as tumor-targeted delivery.

Keywords: tumor targeting, nanoparticles, hyaluronic acid

Introduction

Gambogic acid (GA) is the main active ingredient of gamboge resin that is exuded from the *Garcinia hanburyi* tree in Southeast Asia and has been introduced as an effective anticancer drug.[1,2] GA has shown a broad spectrum of antitumor activity against a wide range of tumor cells such as human gastric carcinoma SGC-7901 cells, human lung carcinoma SPC-A1 cells, and human hepatoma SMMC-7721 cells.[3] This potential anticancer activity in vitro and in vivo is mainly assigned to the downregulation of telomerase activity and induction of the apoptotic process.[2,4] It has been reported that the telomerase inhibition by GA was achieved by repression of hTERT transcriptional activity via c-Myc and posttranslational modification of hTERT via Akt.[5] GA also exhibited its strong antitumor effects via the interruption of steroid receptor coactivator-3.[6] Another study has shown that GA could inhibit survivin activity thereby reversing the resistance of gastric cancer cells to docetaxel.[7] The combination therapies may improve the treatment options for gastric cancer as suggested in the study by Wang et al where GA could attenuate 5-fluorouricil (5-FU)-induced apoptosis by modulating metabolic enzymes of 5-FU. Meanwhile, the combined therapy of GA and 5-FU more effectively inhibited tumor growth in vivo as compared to GA or 5-FU alone.[8] However, several drawbacks such as the poor aqueous solubility; sensitivity to the humidity, temperature, and light; rapid plasma clearance; and wide tissue distribution have a

Correspondence: Jing Yao; Jianping Zhou
State Key Laboratory of Natural Medicines, China Pharmaceutical University, 24 Tongjiaxiang, Nanjing 210009, People's Republic of China
Tel +86 25 8327 1102
Fax +86 25 8330 1606
Email yaoj3@163.com; zhoujpcpu@163.com

great impact on the development of the pharmaceutical preparation and the clinical application of GA.

Currently, polymeric nanoparticles have been widely investigated as drug delivery carriers. The amphiphilic polymers can self-assemble in aqueous medium to form nanoparticles with a core–shell structure, where the inner hydrophobic core incorporates the poorly soluble drugs while the outer hydrophilic shell protects the drug from inactivation in biological environment. These nanoparticles possess many excellent properties such as high drug-loading capacity and improved stability in vivo and in vitro due to low critical aggregation concentration. Our previous study has described that the drug loading (DL) of paclitaxel (PTX)-loaded heparin-based nanoparticles was up to 33%.[9] More notably, polymeric nanoparticles could improve the pharmacokinetic and distribution profile (such as longer blood circulation), reduce side effects, and target tumors by enhanced permeability and retention (EPR) effect-based passive mechanisms.[10–12] Hyaluronic acid (HA) has gained intense attention due to its superior properties and potential as a drug delivery carrier. HA is a water-soluble, biocompatible, and biodegradable linear polysaccharide formed by alternating D-glucuronic acid and *N*-acetyl-D-glucosamine units. Importantly, it can interact with CD44 receptor overexpressed in cancer and facilitate the internalization of HA-based nanoparticles into the tumor cells.[13,14] Many HA derivatives have been developed for tumor-targeting delivery of chemical and genetic drugs.[15,16] These HA-based nanoparticles exhibited significantly enhanced targeting efficiency to the tumor and higher therapeutic efficacy due to the HA-mediated endocytosis. Some studies indicate that HA exhibits strong anticancer activity by inhibiting the metastasis and growth of cancer cells.[17,18] The combination of PTX and HA was shown to achieve additional or synergistic antimetastasis effects.[19] In addition, the outer HA shell in the nanoparticles is capable of evading nonspecific uptake by the reticuloendothelial system, thus enhancing the accumulation of the HA-based nanoparticle in the tumor.[20]

We have successfully synthesized an amphiphilic HA derivative (HRA conjugate) with all-trans retinoic acid (ATRA) as a hydrophobic group as reported in our previous study.[21] In this study, HRA conjugate was used to encapsulate GA by self-assembling into nanoparticles in order to improve the aqueous solubility and in vitro and in vivo properties of GA. Interestingly, ATRA can inhibit the cancer cell proliferation and induce cell differentiation of malignant cells.[22] The combination of ATRA and other cytotoxic drugs such as PTX displayed greater and synergistic antitumor effect.[23] Moreover, ATRA can translocate into the nucleus by binding to specific cytosolic proteins such as cellular retinoic acid binding protein II.[24,25] Therefore, it is expected that HRA conjugate, ATRA-modified HA derivative, will facilitate the delivery of GA to the cell nucleus, while displaying a synergistic antitumor effect for cancer chemotherapy. Also, the chemical incorporation of GA into the conjugate can overcome some drawbacks impeding simultaneous delivery of GA and ATRA, which impact their clinical application, eg, hydrolysis of GA, poor solubility, drug aggregation, and precipitation in biological media, thereby losing their therapeutic activity and increasing the risk of embolism.[26] In this way, GA and ATRA will be loaded simultaneously in a nanocarrier and codelivered into the tumor cell through the combination of HA receptor-mediated endocytosis, EPR effect, and reduced uptake by the reticuloendothelial system (as shown in Figure 1).

In this study, the feasibility of GA-loaded HRA nanoparticles (GA-HRA) for combination cancer chemotherapy was evaluated. GA-HRA was characterized in terms of physicochemical properties, safety after intravenous administration, and in vitro cytotoxicity. In addition, intracellular distribution and the tumor targetability of GA-HRA were also investigated by in vitro cellular uptake and in vivo noninvasive near infrared fluorescence imaging system, respectively. Finally, the therapeutic efficiency of GA-HRA in terms of in vivo antitumor activity was assessed in the tumor-bearing nude mouse model.

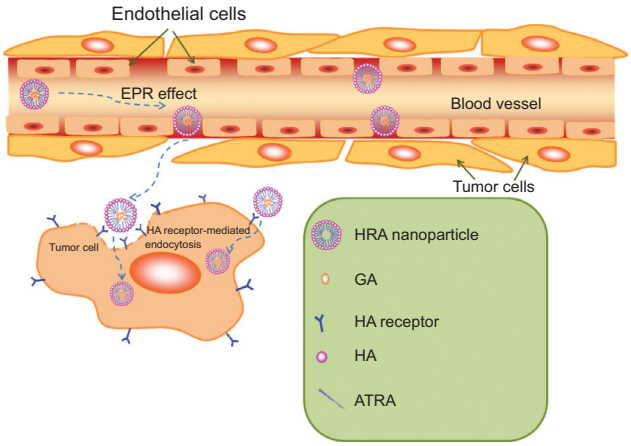

Figure 1 Illustration of the cellular uptake by tumor cells and simultaneous drug delivery of GA-loaded HRA nanoparticles.
Note: The arrows represent the process of HRA delivery into the tumor cells.
Abbreviations: ATRA, all-trans retinoic acid; EPR, enhanced permeability and retention; GA, gambogic acid; HA, hyaluronic acid; HRA, hyaluronic acid-g-all-trans retinoic acid conjugate.

Materials and methods

Materials

Hyaluronic acid (10 kDa) was obtained from Shandong Freda Biochem (Jinan, People's Republic of China). Gambogic acid (GA) and retinoic acid (ATRA) were purchased from Jiangsu Kanion Pharmaceutical (Lianyunguang, People's Republic of China) and Wuhan Hezhong Bio-Chemical Manufacture (Wuhan, People's Republic of China), respectively. Anhydrous dimethylformamide and anhydrous formamide were from Shanghai Lingfeng Chemical Reagent Co. Ltd. (Shanghai, People's Republic of China). 1-Ethyl-3-(3-dimethylaminopropyl)-carbodiimide (EDC) was purchased from Sigma Chemical Co. (St Louis, MO, USA). N-hydroxysuccinimide was from Sinopharm Chemical Reagent Co. (Shanghai, People's Republic of China). All chemicals were of analytical grade and were used without further purification.

Preparation and characterization of HRA conjugate

The HRA conjugate was synthesized as described in our previous study.[21] In brief, aminoethyl ATRA was first synthesized and then reacted with the carboxylic acids of HA in the presence of EDC and N-hydroxysuccinimide. The products were characterized by proton nuclear magnetic resonance (Avace AV-500; Bruker, Ettlingen, Germany). The characteristic peaks of two new amide linkages at 8.01 ppm and 8.35 ppm indicated that ATRA was successfully grafted to the HA structure. The degree of substitution (DS) was estimated by ultraviolet (UV) spectrometry (λ =345 nm).

Preparation and characterization of GA-HRA

The GA-HRA was prepared by a dialysis method. In brief, 330 µL of GA solution in ethanol (27 mg/mL) was slowly added to the HRA solution with stirring. The resulting solution was sonicated for 30 minutes in an in ice bath and dialyzed against water overnight. The dialyzed solution was then centrifuged for 15 minutes at 3,500 rpm, filtered through a 0.45 µm microporous membrane, and lyophilized to obtain the GA-HRA. The amount of the loaded GA in HRA nanoparticles was determined by high performance liquid chromatography (LC-2010 system; Shimadzu, Kyoto, Japan) with UV detection at 360 nm. The separation of analytes was carried out on a LiChrospher C18 column (250 mm×4.6 mm, 5 µm) at 30°C. The mobile phases consisted of 93% methanol and 7% water containing 0.1% acetic acid and was delivered isocratically at a flow rate of 1 mL/min. The DL (%) and entrapment efficiency (%) of GA were calculated as described previously.[9]

The lyophilized nanoparticles were dispersed in 5 mL of 5% glucose solution. The particle size and zeta potential of the nanoparticles were determined by a NanoSight NS500 equipped with the NTA 2.3 analytical software (NanoSight, Amesbury, UK) and dynamic light scattering measurements (BI-200SM; Brookhaven Instruments Corp, Holtsville, NY, USA). The morphology of HRA nanoparticles was observed by scanning probe microscopy (Nanoscope V; Veeco Instruments, Santa Barbara, CA, USA) and transmission electron microscopy (Hitachi H-600; Hitachi Ltd., Tokyo, Japan).

Biocompatibility assessment

Different volumes of drug-free and drug-loaded nanoparticles solution were added into 2% of rabbit red blood cells (RBC) suspension, respectively. Into each tube, 5% glucose injection solution was added to obtain a final volume of 5 mL. In order to eliminate the background effect, 2.5 mL of water (positive control) and 5% glucose injection solution (negative control) were mixed with 2.5 mL of 2% RBC suspension. Samples were then incubated at 37°C for 1 hour, followed by centrifugation at 3,000 rpm for 10 minutes to remove nonlysed RBCs. The degree of hemolysis was determined by spectrophotometry at 540 nm.

The intravenous irritation test was assessed using three rabbits weighing 1.8–2.0 kg. Rabbits were injected with the combination of GA-ATRA-HA solution, HRA conjugate solution, or GA-HRA into the vein at the edge of the left ear for 3 days. As a control, an equivalent volume of 5% glucose solution was injected into the right ear-border vein. The rabbits were then sacrificed 24 hours after the last administration, and the ears were cut followed by fixation in 10% formaldehyde for histological examination.

In vitro cytotoxicity studies

A standard thiazolyl blue tetrazolium bromide (MTT) assay was used to evaluate the cytotoxicity of the nanoparticles. The GA solution and the combination of GA-ATRA-HA solution were used as the positive control. All samples were carried out at equivalent GA and ATRA concentrations. The MCF-7 cells and KB31 cells were seeded at a density of 1×10^4 cells/well in 96-well microtiter plates and incubated at 37°C in a humidified atmosphere with 5% CO_2 for 24 hours. The cells were then treated with different formulations. After incubation for 48 hours, MTT solution (20 µL, 5 mg/mL in phosphate buffered saline [PBS]) was added to each well, and the

cells were further incubated for 4 hours. The media were then removed, and dimethyl sulfoxide was added to dissolve the formazan crystals. The cytotoxic activity was measured by reading the optical density (OD) on a microplate reader at 570 nm wavelength. Cell viability (%) was calculated as OD of test group/OD of control group ×100.

Cellular uptake of HRA nanoparticles

Cellular uptake studies were performed using coumarin-6 dye as fluorescence probe. The coumarin-6-loaded HRA nanoparticles were prepared by the dialysis method. The MCF-7 cells were seeded into a 6-well plate at a density of 1×10^5 cells/well and incubated in the growth medium at 37°C for 24 hours. The growth medium was then replaced with media containing free coumarin-6 solution and coumarin-6-loaded HRA nanoparticles, followed by incubation for 1, 2, and 4 hours. The cells were washed three times with PBS and fixed with 4% paraformaldehyde for 20 minutes, followed by adding Hoechst 33342 (Beyotime Biotechnology, Shanghai, People's Republic of China) to stain the cell nuclei. Finally, the cells were washed twice with PBS (pH 7.4) and observed using a Leica SP5 confocal microscope (excitation λ 495 nm; emission λ 520 nm).

Cells were analyzed by flow cytometry to quantify the cellular uptake of nanoparticles. To investigate whether the process of HA-receptor-mediated endocytosis was involved in the specific uptake of HRA nanoparticles, MCF-7 cells pretreated with or without free HA were incubated with free coumarin-6 solution or coumarin-6-loaded HRA nanoparticles for 6 hours. The uptake efficiency of the nanoparticles was determined through quantification of coumarin-6-positive cells by flow cytometric analysis (BD Biosciences, San Jose, CA, USA).

In vivo imaging analysis

The In-Vivo Imaging System (DXS4000PRO; Kodak, Rochester, NY, USA) was used to monitor the biodistribution of HRA nanoparticles in the tumor-bearing mice. The DiR (1,1′-dioctadecyl-3,3,3′,3′-tetramethylindotricarbocyanine iodide), near-infrared fluorescence dye, was used as a probe. Nine tumor-bearing mice were randomly divided into three groups. The first group was injected intravenously with the saline solution and was used as a control. The two other groups were injected with the same dose of DiR (5 mg/mL) in free DiR solution and DiR-loaded HRA nanoparticles (n=3 for each group). Imaging was performed at 1, 4, 8, and 24 hours after injection to estimate the time-correlated excretion profile. The image analysis was performed using the Kodak Molecular Imaging Software 5.X.

In vivo antitumor activity

In vivo antitumor activity of the nanoparticles was evaluated in the subcutaneous MCF-7 tumor-bearing nude mouse model. When the tumor volume reached approximately 100 mm^3, mice were randomly divided into four groups (n=5 for each group) to receive intravenous injection of normal saline (control group), GA solution (8 mg GA/kg), the combination of GA-ATRA-HA solution (8 mg/kg GA and 2.1 mg/kg ATRA), and GA-HRA (8 mg/kg GA and 2.1 mg/kg ATRA-equivalent). A mixture containing equal volumes of ethanol and cremophor EL was used as solvent for the two free drug groups. The therapy was continued six times at 2-day intervals through tail vein injection. The antitumor activity of the tested formulations was estimated by recording the changes in tumor mass. Tumor volumes were monitored by recording the tumor length and width with a caliper then calculated using the equation,

$$V = 0.5 \times a \times b^2 \quad (1)$$

where V is tumor volume (mm^3), a is tumor length (mm), and b is tumor width (mm). Mice were sacrificed on the 12th day after administration, and the tumors were weighed. Furthermore, in vivo tumor cell apoptosis was investigated using the terminal deoxynucleotidyl transferase dUTP nick end labeling (TUNEL) assay and hematoxylin and eosin staining assay. TUNEL staining was conducted according to the manufacturer's recommendations, and nuclear staining was performed using 4′,6-diamino-2-phenylindole mounting medium.

Statistical analysis

Data are expressed as mean ± standard deviation. The two-way unweighted mean analysis of variance (ANOVA) test was used to determine the statistical significance, and a value of $P<0.05$ was considered significant.

Results and discussion

Preparation and characterization of GA-HRA

In this study, hydrophobic ATRA was conjugated to water-soluble HA backbone to get the amphiphilic HRA polymer (Figure 2A). Such polymers can self-assemble into nanoparticles in aqueous medium for loading the hydrophobic drugs. The degree of ATRA substitution in the HA molecule (DS) could be controlled in the range of 5.1–11.8 wt% by varying the molar ratio of aminoethyl ATRA to the carboxylic acid of HA. Previous reports have suggested that high DS

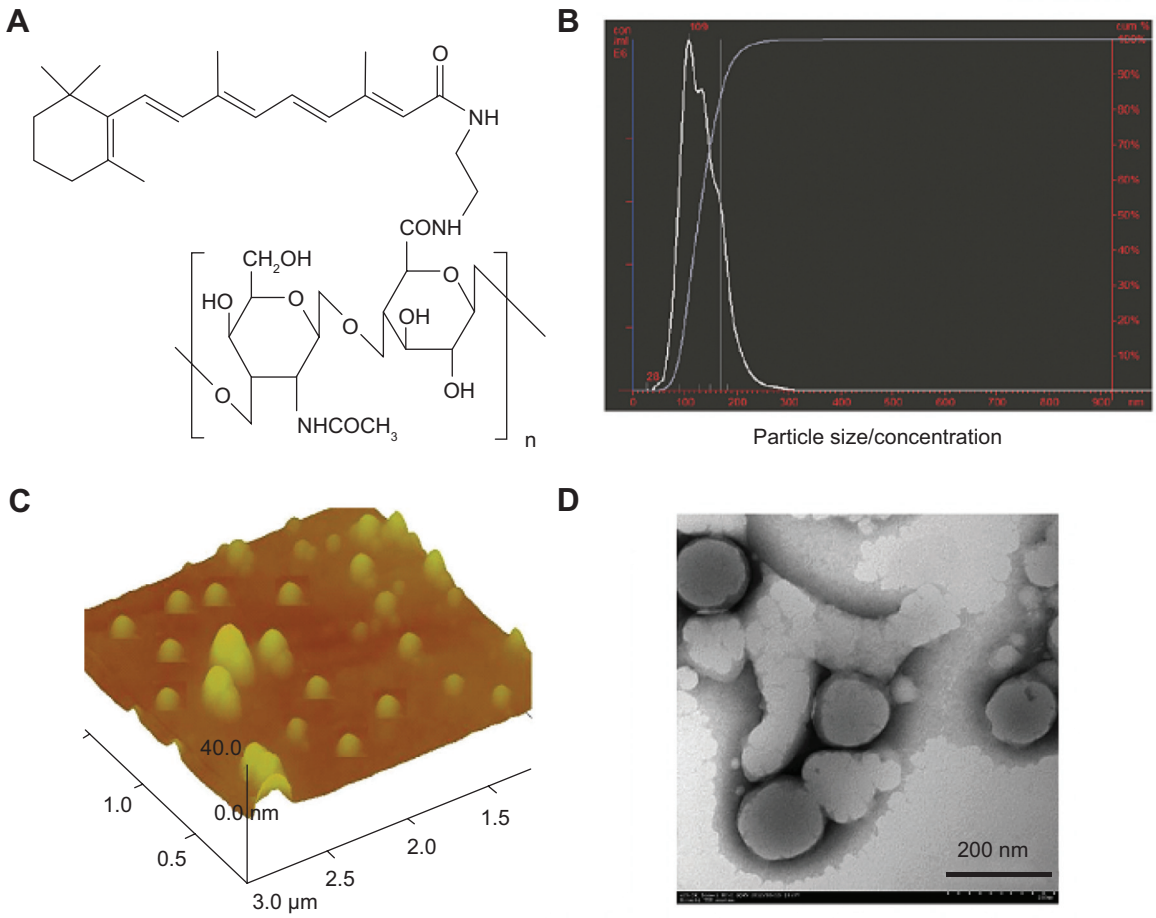

Figure 2 Chemical structure of hyaluronic acid-g-all-trans retinoic acid (HRA) conjugate (**A**); mean particle size of GA-loaded HRA nanoparticles (GA-HRA) determined by a NanoSight NS500 (**B**); atomic force microscopy images (**C**); and transmission electron microscopy images of GA-HRA (**D**).
Abbreviation: GA, gambogic acid.

would contribute to high DL as a result of the hydrophobic interactions between loaded drugs and the hydrophobic core ATRA of the conjugate.[9,27,28] Therefore, HRA conjugate with a high DS of 11.8 wt% was selected as the representative candidate for further studies.

The in vivo behavior of nanoparticles is greatly influenced by their particle size and distribution. The mean particle size of GA-HRA was 134±36 nm, with narrow size distribution (Figure 2B), which will benefit the uptake of nanoparticles by tumor cells due to EPR effect.[29,30] Moreover, the particle sizes of GA-HRA were bigger than those of unloaded HRA nanoparticles, probably because the bulk drugs enlarged the hydrophobic core of nanoparticles (data not shown). The unloaded and GA-loaded polymeric nanoparticles were negatively charged (approximately −30 mV), owing to the negatively charged carboxyl groups of HA, which form the outer shell to increase the nanoparticles' stability. In addition, the nanoparticle had high DL% (31.1%) and entrapment efficiency (90.5%) as expected, which further confirm that amphiphilic polymer is an excellent carrier for hydrophobic drugs.[9] The representative atomic force microscopy and transmission electron microscopy images of the nanoparticles are shown in Figure 2C and D. The results showed that the GA-HRA were spherical in shape with uniform size distribution.

Biocompatibility

In the study, the hemolysis and intravenous irritation were performed in order to assess the feasibility of HRA nanoparticles for intravenous administration. As shown in Figure 3A, GA-HRA displayed almost no hemolytic effect, suggesting that GA-HRA was not toxic towards erythrocytes. On the contrary, the hemolysis of GA plus ATRA solution reached 44.5% at 0.2 mg/mL concentration, indicating that the drug encapsulation into nanoparticles would improve the drug biocompatibility by blocking the direct contact of drugs with erythrocytes, as suggested in previous studies[9,31] where low molecular weight heparin-ATRA conjugate and *N*-octyl-*O*, *N*-carboxymethyl chitosan significantly decreased the hemolytic activity of

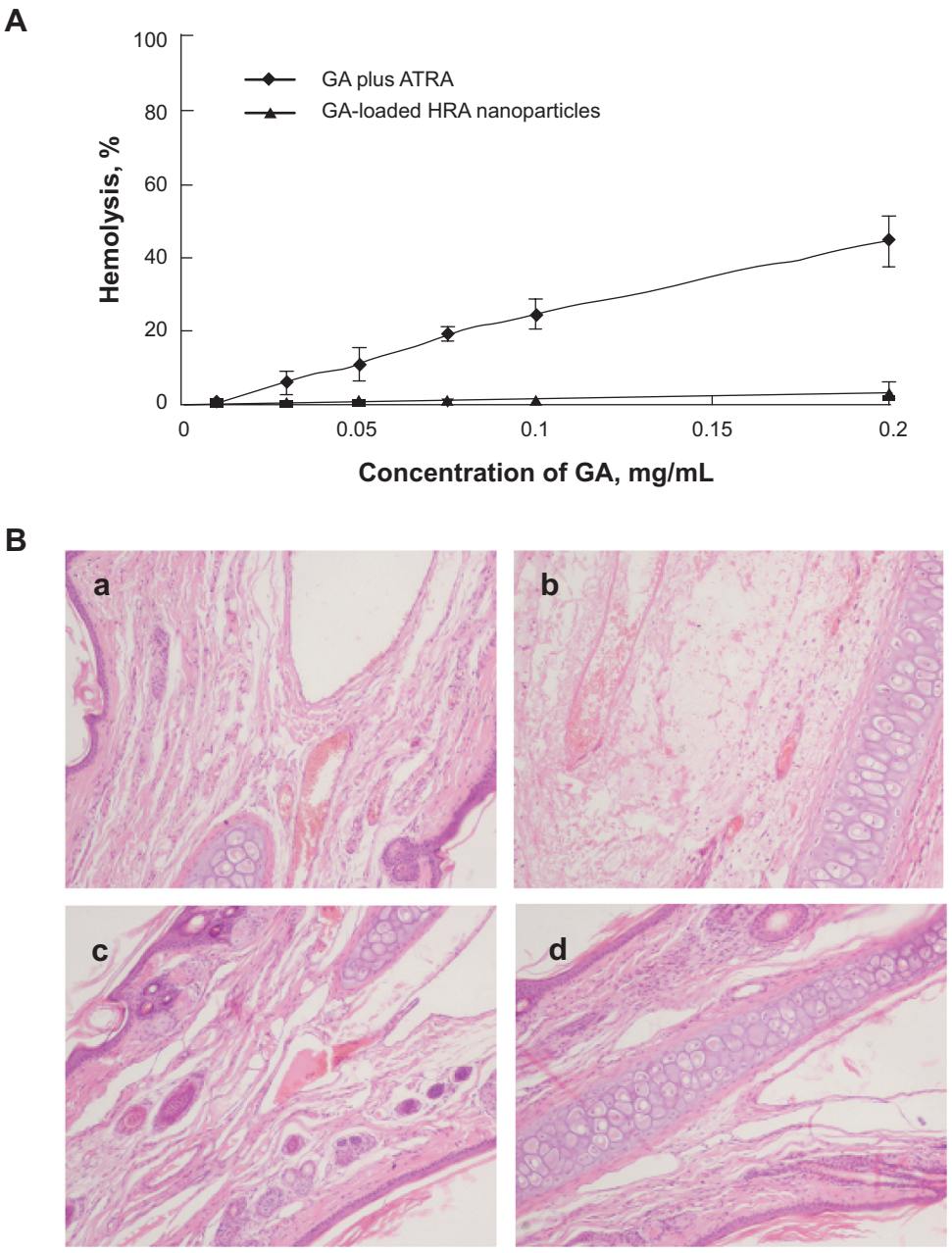

Figure 3 Safety evaluation of HRA nanoparticles.
Notes: Hemolysis as a function of vehicle concentration of HRA conjugate and GA-HRA (n=3) (**A**); pathological section of vessel tissues (**B**); control (5% glucose solution) (**a**); combination of GA-ATRA-HA solution (**b**); HRA conjugate (**c**); GA-HRA (**d**).
Abbreviations: ATRA, all-trans retinoic acid; GA, gambogic acid; GA-HRA, GA-loaded HRA nanoparticles; HA, hyaluronic acid; HRA, hyaluronic acid-g-all-trans retinoic acid.

PTX solution. In addition, HRA conjugate also did not cause hemolysis with the range of equivalent doses.[21]

As shown in Figure 3B, the histopathologic examination of the rabbit ear-border vein after a 3-day administration of GA-HRA showed no angiectasia or thrombus formation in the vein lumen, similarly to the control group and the HRA conjugate group. In addition, no erythema or edema response was noticed in the rabbit ears after multidose administration, unlike GA solution where serious intravenous irritation was observed. These results showed that GA-HRA and HRA conjugate did not cause any simulative reaction in the rabbit's ear vein. Therefore, based on the hemolysis and intravenous irritation test, GA-HRA exhibited better biocompatibility compared to the GA solution.

In vitro cytotoxicity studies

The cytotoxicity of GA-HRA was investigated in MCF-7 cells and KB31 cells by the MTT assay. The tumor cells

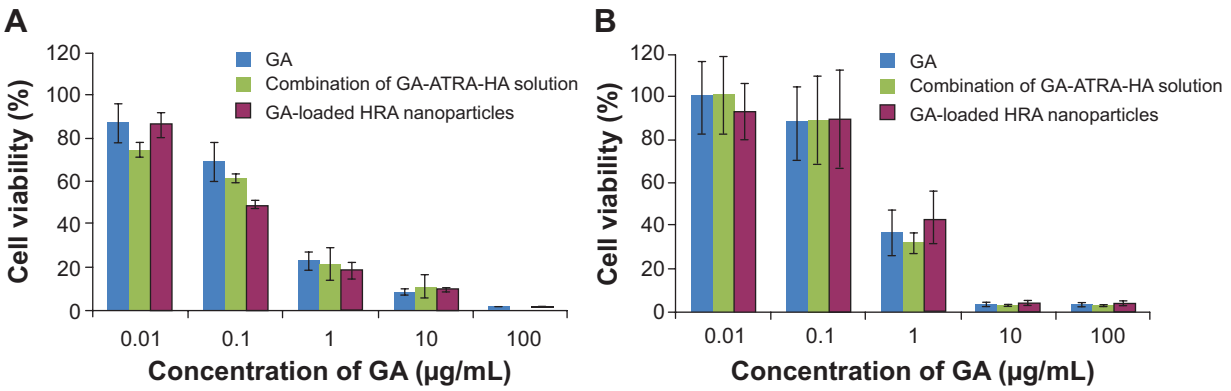

Figure 4 Viability of MCF-7 cells (**A**) and KB31 cells (**B**) as a function of GA concentration for GA solution, GA-HRA, and the combination of GA-ATRA-HA solution.
Notes: Cell survival fractions were assessed by MTT assay; data represent mean ± SD (n=5).
Abbreviations: ATRA, all-trans retinoic acid; GA, gambogic acid; GA-HRA, GA-loaded HRA nanoparticles; HA, hyaluronic acid; HRA, hyaluronic acid-g-all-trans retinoic acid; MTT, thiazolyl blue tetrazolium bromide; SD, standard deviation.

were treated with the GA solution, the combination of GA-ATRA-HA solution, and GA-HRA (at the equivalent GA and ATRA concentrations) for 48 hours. As illustrated in Figure 4, three groups showed a typical concentration-dependent cytotoxicity. The half maximal inhibitory concentration (IC_{50}) values in MCF-7 cells were 0.219 μg/mL, 0.131 μg/mL, and 0.126 μg/mL for the GA solution, the combination of GA-ATRA-HA solution, and GA-HRA, respectively. Based on the cell viability and IC_{50} values, the combination of GA-ATRA-HA solution achieved a better cytotoxic effect than GA solution, indicating that the combination of GA, ATRA, and HA was more effective in killing the tumor cells. Notably, GA-HRA showed a comparable cell growth inhibition effect on the MCF-7 cells as compared to the combination of GA-ATRA-HA solution. Moreover, KB31 cells showed no significant difference in viability between the three formulations. In general, the nanoparticles were less toxic than free drugs due to a lower concentration gradient under in vitro conditions, which might be explained by the delayed drug release from nanoparticles.[32,33] In the present study, the enhanced cellular uptake by HA receptor-mediated endocytosis mainly contributed to higher cytotoxicity of GA-HRA than usual, as suggested in previous studies, where doxorubicin-loaded octreotide-modified polymeric micelles exhibited stronger cytotoxicity against MCF-7 cells compared to free doxorubicin.[34] Consequently, the entrapment of GA into the HRA nanoparticles improved its stability in the medium by protecting the drug from epimerization and hydrolysis, thereby enhancing the therapeutic activity.

We investigated in vitro release of GA from HRA nanoparticles after 72 hours' incubation in PBS buffer (pH =7.4) containing 0.2% Tween 80. Only 11% of the initially loaded GA was released after 72 hours. Therefore, taking into account the sustained drug-release characteristics of nanoparticle-based formulations, it could be concluded that GA-HRA might kill the cancer cells more effectively compared to free drugs. It could also be expected that GA-HRA would be more effective during circulation in vivo due to the targeting ability of HA.[35]

Moreover, HRA conjugate showed no cytotoxicity at investigated concentrations ranging from 0.01 μg/mL to 100 μg/mL equivalent to the amount of the conjugate in GA-HRA. Considering the above results (hemolysis, intravenous irritation, and cytotoxicity studies), it might be concluded that HRA conjugate can be used as a safe intravenous injectable nanocarrier for antitumor drugs.

Cellular uptake of the HRA nanoparticles

The therapeutic efficacy of the encapsulated drug in nanoparticles is usually directly influenced by the cellular uptake and distribution of the nanoparticles, and thus, a high binding affinity of the nanoparticles to tumor cells remains essential for efficient accumulation at the tumor site to achieve the intended therapeutic effect.[36]

Previous studies have demonstrated that HA-based nanoparticles showed high cell uptake efficiency by receptor-mediated active targeting mechanism.[14,15,37] In this study, the intracellular distribution of HRA nanoparticles in MCF-7 cells was monitored by confocal laser scanning microscopy. The coumarin-6, as a fluorescent marker, was encapsulated into HRA nanoparticles. Moreover, the nuclei of cells were stained with Hoechst 33342 to visualize the distribution of nanoparticles. Figure 5A shows the confocal microscopic images of MCF-7 cells treated with free coumarin-6 (as the control) and coumarin-6-loaded HRA nanoparticles at different incubation times. In the case of

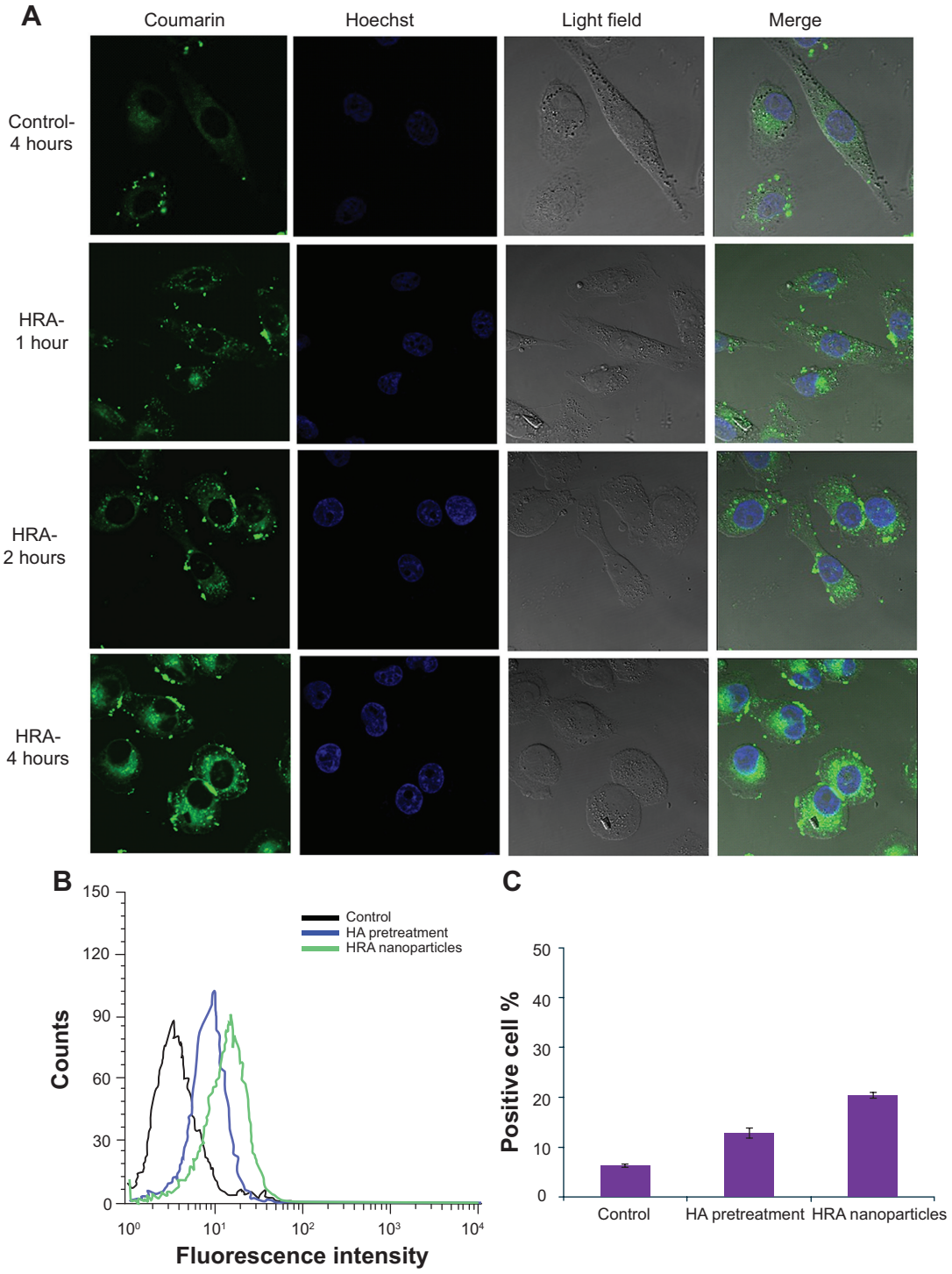

Figure 5 Cellular uptake.
Notes: Confocal microscopic images of MCF-7 cells after incubation with free coumarin-6 for 4 hours and with coumarin-6-loaded HRA nanoparticles for 1 hour, 2 hours, and 4 hours, respectively (**A**); FACS graphs of fluorescence accumulation in MCF-7 cells (**B**); positive cell percent age demonstrated by flow cytometry (**C**); results were expressed as mean ± SD (n=3).
Abbreviations: FACS, fluorescence-activated cell sorting; HA, hyaluronic acid; HRA, hyaluronic acid-g-all-trans retinoic acid; SD, standard deviation.

HRA nanoparticles, the fluorescence signal gradually became stronger with extended incubation time. In particular, HRA nanoparticles showed a well-distributed green fluorescence in the cytoplasm at 4 hours, which was significantly stronger than free coumarin-6. This might be attributed to the HA receptor-mediated endocytosis through the preferential binding of HA to HA receptor, which is highly expressed on the surface of tumor cells. More interestingly, although

coumarin-6-loaded HRA nanoparticles were mainly localized in the cytoplasm, similarly to most polymers and nanoparticles,[37,38] much stronger green fluorescence appeared in the nuclei compared to the control and exhibited time-dependent distribution properties. This might be associated with ATRA-induced nuclear translocation as well as higher cellular uptake efficiency of HA-mediated endocytosis. The former may contribute to the enhanced nucleus delivery of HRA nanoparticles due to the nuclear translocation of ATRA after binding to specific cytosolic proteins such as cellular retinoic acid-binding protein II and FABP5 (fatty acid binding protein-5), as suggested in a previous report.[39] Moreover, a low intensity signal had been observed after 1 hour incubation with HRA nanoparticles, indicating the rapid internalization and nuclear transport of the nanoparticles.

Next, a competitive inhibition experiment was performed to confirm the uptake of the nanoparticles by HA receptor-mediated endocytosis. HA receptors were saturated by incubating the cancer cells with free HA at 5 mg/mL for 1.5 hours before adding the formulations. The fluorescence intensity in MCF-7 cells was quantitatively measured by flow cytometry (as shown in Figure 5B and C). The cells treated with free fluorescence probe were used as the control. As expected, positive cell percentage was significantly reduced after the pretreatment of the MCF-7 cells with free HA ($P<0.05$), indicating that the efficient cellular uptake of HRA nanoparticles was attributed to the HA receptor-mediated endocytosis. In addition, we also found that the cellular uptake of HRA nanoparticles was much greater than that of the control ($P<0.01$) (3.5 times higher), in accordance with the confocal laser scanning microscopic observations.

In vivo imaging analysis

The biodistribution and tumor targeting efficiency of HRA nanoparticles in tumor-bearing mice were investigated by the In Vivo Images System. Figure 6 shows the real-time images of DiR-labeled HRA nanoparticles and free DiR (as the control) in tumor-bearing mice. The results indicated that free DiR was distributed in tumor-bearing mice quickly, and the fluorescent signal was the strongest at 1 hour. Subsequently, the fluorescent intensity gradually decreased, then disappeared completely at 24 hours. However, DiR-loaded HRA nanoparticles showed much stronger fluorescent signals than free DiR at any time of postinjection, from 4 hours to 24 hours. In particular, they kept a long-lasting and strong fluorescence signal from 4 hours to 8 hours while the signal was still obviously observed up to 24 hours. Accordingly, it was suggested that HRA nanoparticles might facilitate the delivery of antitumor drugs into the tumor with long-term retention in the tumor, which would enhance the antitumor effect.

Different in vivo fates of free DiR and DiR-loaded HRA nanoparticles might result from their different biodistribution mechanisms. Free DiR is a low molecular weight substance that can be distributed systemically in the body and transported across cellular membrane by passive diffusion, which resulted in its low uptake in the tumor site, as expected, owing to the low concentration gradient. However, as suggested by the cell uptake study, HRA nanoparticles were mainly internalized by tumor cells through HA receptor-mediated endocytosis. Moreover, small particle sizes of HRA nanoparticles (<200 nm) have also contributed to the efficient cell uptake and long-term retention in the tumor site through the typical EPR effect.[29] Therefore, HRA nanoparticles showed an extended circulation profile with better tumor accumulation than free DiR.

In vivo antitumor activity

The in vivo antitumor efficacy was investigated after repeated intravenous administration to further confirm the antitumor potential of GA-HRA. Saline solution was used as the negative control, and the GA solution and the combination of GA-ATRA-HA solution served as the positive control. As illustrated in Figure 7, compared to the control group, three treatment groups showed obvious tumor growth inhibition activity. In particular, the tumor volumes in the GA-HRA group were much smaller than those of the GA solution group ($P<0.01$) and the combination of GA-ATRA-HA solution group ($P<0.05$), indicating a statistically improved antitumor effect of GA-HRA compared to two free drugs groups. Similarly, the tumor weights of mice treated with GA-HRA were significantly decreased compared to other formulations (data not shown). Moreover, the combination of GA-ATRA-HA solution induced slower tumor growth than the GA solution, indicating an effective synergetic antitumor activity. Good in vivo efficacy of GA-HRA were involved in its successful delivery to the tumor site depending on the nanoparticle vector. It is well known that HA-based nanoparticles facilitate targeted delivery of drugs into the tumor by HA receptor-mediated endocytosis as well as EPR effect and extended blood circulation time,[29,30,37] which would benefit the enhanced in vivo efficacy of antitumor drugs. In addition, HRA nanoparticles conferred good aqueous solubility and stability to GA and ATRA in the circulatory system, which may facilitate their clinical application. More interestingly, they could simultaneously

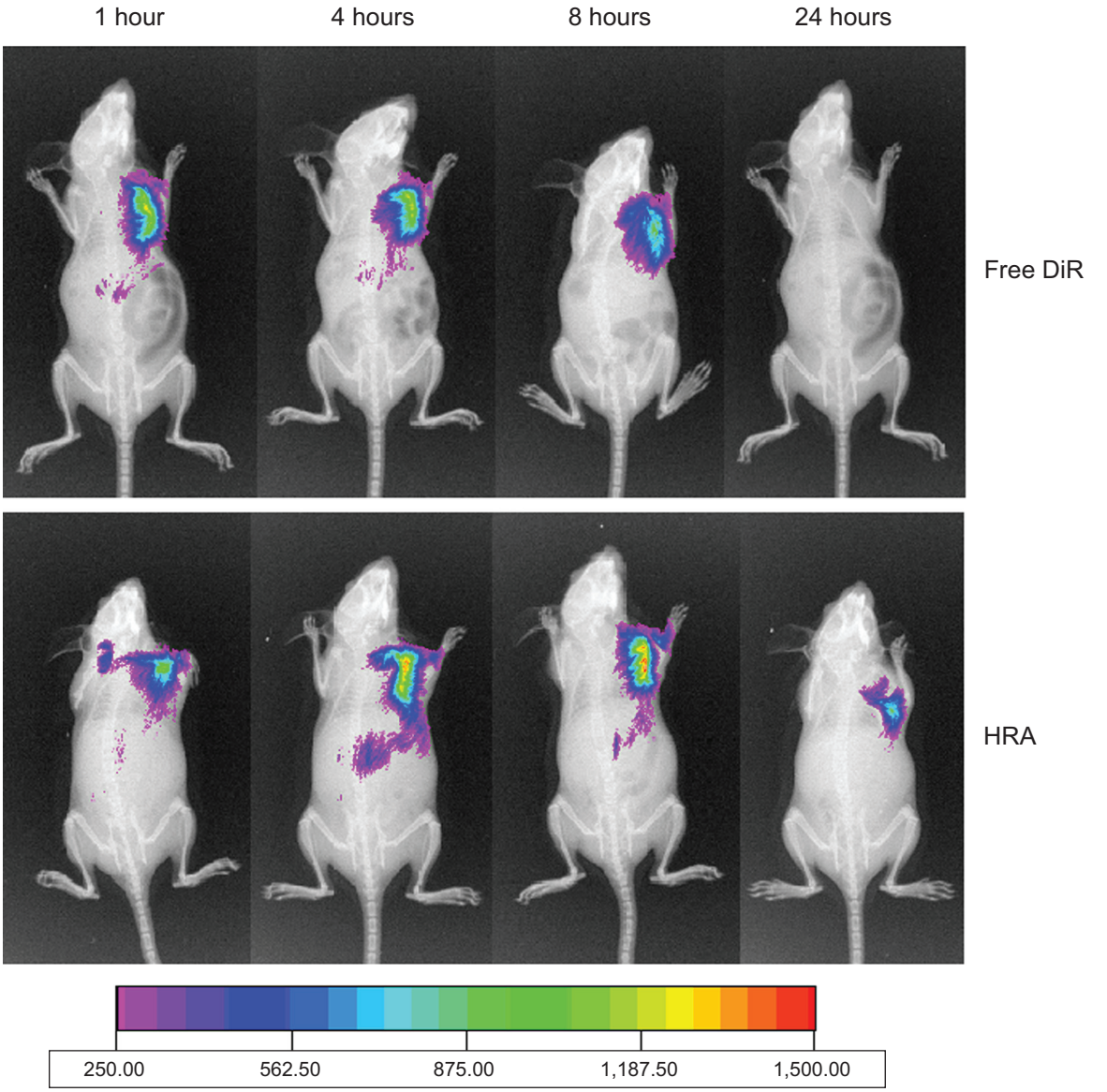

Figure 6 Typical in vivo noninvasive fluorescence images of tumor-bearing mice at 1 hour, 4 hours, 8 hours, and 24 hours after intravenous injection of DiR-loaded HRA nanoparticles and free DiR.
Note: The NIR fluorescence images and X-ray images were fused together with Kodak Molecular Image Systems software V 5.0.1.
Abbreviations: HRA, hyaluronic acid-g-all-trans retinoic acid; NIR, near infrared; DiR, 1,1′-dioctadecyl-3,3,3′,3′-tetramethylindotricarbocyanine iodide.

deliver GA and ATRA to the tumor, which would contribute to the improved antitumor effect of the combination therapy. In contrast, free drugs usually exhibit little drug accumulation at the tumor site due to rapid clearance and nonspecific distribution after intravenous administration.

The improved antitumor activity of GA-HRA was further confirmed by DNA fragmentation in tumor cells after TUNEL staining. As shown in Figure 7C, a greater induction of tumor cell apoptosis was observed with GA-HRA compared to other groups. In addition, GA-HRA resulted in the most severe tumor necrosis compared to other formulations. These results further suggest the outstanding antitumor efficacy of GA-HRA.

The potential toxicity of polymeric nanoparticles should be considered for their clinical application. The change in mouse body weight and status were recorded to evaluate the toxicity of nanoparticles. As shown in Figure 7B, there was no obvious body weight loss in mice after intravenous administration of GA-HRA ($P<0.05$). However, the body weight of the mice in the GA solution group and the combination of GA-ATRA-HA solution group were significantly decreased, with noticeable activity change within the first few minutes after administration ($P<0.01$). Therefore, GA-HRA was considered to be much safer than other formulations, so it may also be concluded that HRA nanoparticles are essential to improve the toxicity of GA as well as its in vivo efficacy.

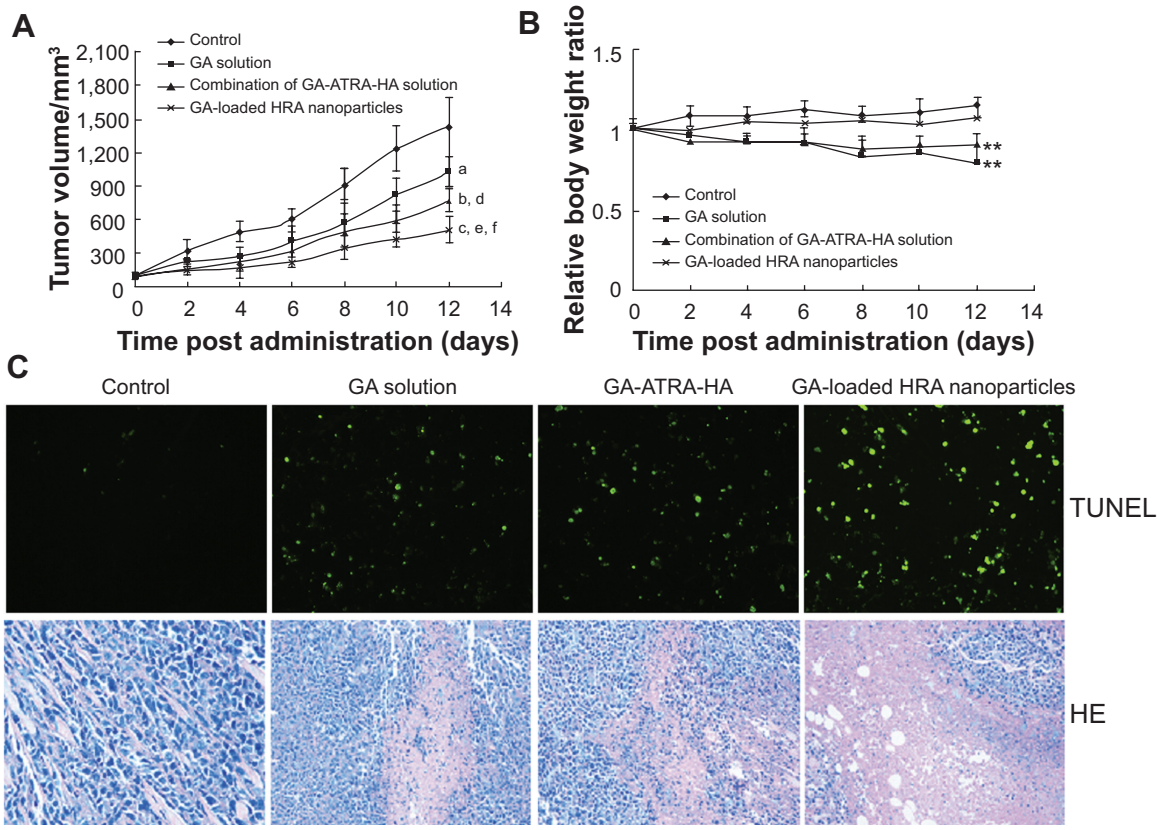

Figure 7 In vivo efficacy assay of GA-HRA.

Notes: Tumor growth kinetics with dosing every other day for 6 times (**A**); data are expressed as mean ± SD (n=5); $^{a}P<0.05$, $^{b}P<0.01$, and $^{c}P<0.001$ versus the control, $^{d}P<0.05$ and $^{e}P<0.01$ versus GA solution, $^{f}P<0.05$ versus combination of GA-ATRA-HA solution; relative body weight ratio of tumor-bearing mice after the treatment (**B**); data are expressed as mean ± SD (n=5); $^{**}P<0.01$ versus control; representative images of paraffin-embedded tumor sections after TUNEL (the apoptotic cells shown in green) and HE staining (**C**).

Abbreviations: ATRA, all-trans retinoic acid; GA, gambogic acid; GA-HRA, GA-loaded HRA nanoparticles; HA, hyaluronic acid; HE, hematoxylin and eosin; HRA, hyaluronic acid-g-all-trans retinoic acid; SD, standard deviation; TUNEL, terminal deoxynucleotidyl transferase dUTP nick end labeling.

Conclusion

In this study, GA-HRA was prepared to facilitate the simultaneous delivery of GA and ATRA to tumor cells. GA-HRA exhibited high DL (over 30%), a particle size of less than 150 nm, and good biocompatible characteristics. HRA nanoparticles could be efficiently taken up by MCF-7 cells and translocated into the nucleus in a time-dependent manner. Moreover, HRA nanoparticles showed prolonged circulation time and preferential accumulation at the tumor site compared to the free DiR solution. More importantly, the administration of GA-HRA resulted in a significant reduction of tumor volume and systemic side effects such as animal weight loss, suggesting an excellent in vivo antitumor efficacy with less toxicity. In conclusion, GA and ATRA can successfully realize a effective combination chemotherapy as well as tumor-targeted delivery with the help of HRA nanoparticles.

Acknowledgments

This work was supported by the National Natural Science Foundation of China (No 81173006), the Project Program of State Key Laboratory of Natural Medicines, China Pharmaceutical University (No JKGQ201107), the Jiangsu Natural Science Foundation of China (SBK201322347), Qing Lan Project, the Fundamental Research Funds for the Central Universities (JKPZ2013005), and Jiangsu Overseas Research and Training Program for University Prominent Young and Middle-aged Teachers and Presidents.

Disclosure

The authors report no conflicts of interest in this work.

References

1. Auterhoff H, Frauendorf H, Liesenklas W, Schwandt C. [The chief constituents of gamboge resins. 1. Chemistry of gamboge]. *Arch Pharm.* 1962;295/67:833–846. German.
2. Wang X, Deng R, Lu Y, et al. Gambogic acid as a non-competitive inhibitor of ATP-binding cassette transporter B1 reverses the multidrug resistance of human epithelial cancers by promoting ATP-binding cassette transporter B1 protein degradation. *Basic Clin Pharmacol Toxicol*. 2013; 112(1):25–33.
3. Wang J, Ma J, You Q, et al. Studies on chemical modification and biology of a natural product, gambogic acid (II): synthesis and bioevaluation of gambogellic acid and its derivatives from gambogic acid as antitumor agents. *Eur J Med Chem*. 2010;45(9):4343–4353.

4. Qi Q, You Q, Gu H, et al. Studies on the toxicity of gambogic acid in rats. *J Ethnopharmacol*. 2008;117(3):433–438.
5. Zhao Q, Yang Y, Yu J, et al. Posttranscriptional regulation of the telomerase hTERT by gambogic acid in human gastric carcinoma 823 cells. *Cancer Lett*. 2008;262(2):223–231.
6. Li R, Chen Y, Zeng LL, et al. Gambogic acid induces G0/G1 arrest and apoptosis involving inhibition of SRC-3 and inactivation of Akt pathway in K562 leukemia cells. *Toxicology*. 2009;262(2):98–105.
7. Wang T, Wei J, Qian X, Ding Y, Yu L, Liu B. Gambogic acid, a potent inhibitor of survivin, reverses docetaxel resistance in gastric cancer cells. *Cancer Lett*. 2008;262(2):214–222.
8. Wang J, Liu W, Zhao Q, et al. Synergistic effect of 5-fluorouracil with gambogic acid on BGC-823 human gastric carcinoma. *Toxicology*. 2009;256(1–2):135–140.
9. Hou L, Fan Y, Yao J, et al. Low molecular weight heparin-all-trans retinoic acid conjugate as a drug carrier for combination cancer chemotherapy of paclitaxel and all-trans retinoic acid. *Carbohyd Polym*. 2011;86(3):1157–1166.
10. Kwon GS, Okano T. Polymeric micelles as new drug carriers. *Adv Drug Deliv Rev*. 1996;21(2):107–116.
11. Gaucher G, Dufresne MH, Sant VP, Kang N, Maysinger D, Leroux JC. Block copolymer micelles: preparation, characterization and application in drug delivery. *J Control Release*. 2005;109(1–3):169–188.
12. He M, Zhao Z, Yin L, Tang C, Yin C. Hyaluronic acid coated poly(butyl cyanoacrylate) nanoparticles as anticancer drug carriers. *Int J Pharm*. 2009;373(1–2):165–173.
13. McKee MC, Lowenstein CJ, Horton MR, et al. Hyaluronan fragments induce nitric-oxide synthase in murine macrophages through a nuclear factor kappB-dependent mechanism. *J Biol Chem*. 1997;272(12):8013–8018.
14. Nedvetzki S, Gonen E, Assayag N, et al. RHAMM, a receptor for hyaluronan-mediated motility, compensates for CD44 in inflamed CD44-knockout mice: a different interpretation of redundancy. *Proc Natl Acad Sci U S A*. 2004;101(52):18081–18086.
15. Ito T, Iida-Tanaka N, Koyama Y. Efficient in vivo gene transfection by stable DNA/PEI complexes coated by hyaluronic acid. *J Drug Target*. 2008;16(4):276–281.
16. Yao J, Fan Y, Du R, et al. Amphoteric hyaluronic acid derivative for targeting gene delivery. *Biomaterials*. 2010;31(35):9357–9365.
17. Tan B, Wang JH, Wu QD, Kirwan WO, Redmond HP. Sodium hyaluronate enhances colorectal tumour cell metastatic potential in vitro and in vivo. *Br J Surg*. 2001;88(2):246–250.
18. Jiang G, Park K, Kim J, et al. Hyaluronic acid-polyethyleneimine conjugate for target specific intracellular delivery of siRNA. *Biopolymers*. 2008;89(7):635–642.
19. Yin DS, Ge ZQ, Yang WY, Liu CX, Yuan YJ. Inhibition of tumor metastasis in vivo by combination of paclitaxel and hyaluronic acid. *Cancer Lett*. 2006;243(1):71–79.
20. Choi KY, Saravanakumar G, Park JH, Park K. Hyaluronic acid-based nanocarriers for intracellular targeting: interfacial interactions with proteins in cancer. *Colloids Surf B Biointerfaces*. 2012;99:82–94.
21. Yao J, Zhang L, Zhou J, Liu H, Zhang Q. Efficient simultaneous tumor targeting delivery of all-trans retinoic acid and Paclitaxel based on hyaluronic acid-based multifunctional nanocarrier. *Mol Pharm*. 2013;10(3):1080–1091.
22. Ortiz MA, Bayon Y, Lopez-Hernandez FJ, Piedrafita FJ. Retinoids in combination therapies for the treatment of cancer: mechanisms and perspectives. *Drug Resist Updat*. 2002;5(3–4):162–175.
23. Karmakar S, Banik NL, Ray SK. Combination of all-trans retinoic acid and paclitaxel-induced differentiation and apoptosis in human glioblastoma U87MG xenografts in nude mice. *Cancer*. 2008;112(3):596–607.
24. Schug TT, Berry DC, Shaw NS, Travis SN, Noy N. Opposing effects of retinoic acid on cell growth result from alternate activation of two different nuclear receptors. *Cell*. 2007;129(4):723–733.
25. Sessler RJ, Noy N. A ligand-activated nuclear localization signal in cellular retinoic acid binding protein-II. *Mol Cell*. 2005;18(3):343–353.
26. Bae Y, Diezi TA, Zhao A, Kwon GS. Mixed polymeric micelles for combination cancer chemotherapy through the concurrent delivery of multiple chemotherapeutic agents. *J Control Release*. 2007;122(3):324–330.
27. Allen C, Maysinger D, Eisenberg A. Nano-engineering block copolymer aggregates for drug delivery. *Colloid Surface B*. 1999;16(1–4):3–27.
28. Dahmani FZ, Yang H, Zhou J, Yao J, Zhang T, Zhang Q. Enhanced oral bioavailability of paclitaxel in pluronic/LHR mixed polymeric micelles: preparation, in vitro and in vivo evaluation. *Eur J Pharm Sci*. 2012;47(1):179–189.
29. Kohane DS. Microparticles and nanoparticles for drug delivery. *Biotechnol Bioeng*. 2007;96(2):203–209.
30. Yang C, Tan JPK, Cheng W, et al. Supramolecular nanostructures designed for high cargo loading capacity and kinetic stability. *Nano Today*. 2010;5:515–523.
31. Huo MR, Zhang Y, Zhou JP, Lü L, Liu H, Liu FJ. Solubilizing and sustained-releasing abilities and safety preliminary evaluation for paclitaxel based on N-octyl-O, N-carboxymethyl chitosan polymeric micelles. *Yao Xue Xue Bao*. 2008;43:855–861.
32. Park K, Lee GY, Kim YS, et al. Heparin-deoxycholic acid chemical conjugate as an antitumor drug carrier and its antitumor activity. *J Control Release*. 2006;114(3):300–306.
33. Min KH, Park K, Kim YS, et al. Hydrophobically modified glycol chitosan nanoparticles-encapsulated camptothecin enhance the drug stability and tumor targeting in cancer therapy. *J Control Release*. 2008;127(3):208–218.
34. Huo M, Zou A, Yao C, et al. Somatostatin receptor-mediated tumor-targeting drug delivery using octreotide-PEG-deoxycholic acid conjugate-modified N-deoxycholic acid-O, N-hydroxyethylation chitosan micelles. *Biomaterials*. 2012;33(27):6393–6407.
35. Jung B, Jeong YC, Min JH, et al. Tumor-binding prodrug micelles of polymer–drug conjugates for anticancer therapy in HeLa cells. *J Mater Chem*. 2012;22(18):9385–9394.
36. Sugahara KN, Teesalu T, Karmali PP, et al. Coadministration of a tumor-penetrating peptide enhances the efficacy of cancer drugs. *Science*. 2010;328(5981):1031–1035.
37. Upadhyay KK, Bhatt AN, Mishra AK, et al. The intracellular drug delivery and antitumor activity of doxorubicin loaded poly(gamma-benzyl L-glutamate)-b-hyaluronan polymersomes. *Biomaterials*. 2010;31(10):2882–2892.
38. Zhou D, Hu L, Wang W, Zhao X. Cellular uptake of tailored copolymer synthesized via reversible addition-fragmentation chain transfer (RAFT) polymerization. *React Funct Polym*. 2012;72(6):402–406.
39. Hou L, Yao J, Zhou J, Zhang Q. Pharmacokinetics of a paclitaxel-loaded low molecular weight heparin-all-trans retinoic acid conjugate ternary nanoparticulate drug delivery system. *Biomaterials*. 2012;33(21):5431–5440.